ISSN No: 2348-4845
International Journal & Magazine of Engineering, Technology, Management and Research
A Peer Reviewed Open Access International Journal

The Result of Confinement on Dynamic Response of Lean-Premixed Swirl-Stabilized Flame and the Structure of Overall Flames

R.Vedaprahlad
HOD,
Department of Mechanical Engineering,
Avanthi Institute of Engineering and Technology, Hyderabad -500078, India.

ABSTRACT:

In this present paper regarding the combustion instability is a process which involves unsteady chemical kinetic, fluid mechanic, and acoustic processes. It can lead to unstable behavior and be detrimental in ways ranging from faster part fatigue to catastrophic system failure. The effect of flame–wall interactions on the forced response of a lean-premixed, swirl-stabilized flame is experimentally investigated by examining flames in a series of three combustors, each with a different diameter, and therefore a different degree of lateral confinement. The confinement ratios tested are 0.5, 0.37, and 0.29 when calculated using the diameter of the nozzle relative to the combustor diameter. Using both flame images and measured flame transfer functions (FTFs), the effect of confinement is investigated and generalized across a broad range of operating conditions In terms of combustion methodology, combustion instability has been a key issue for lean premixed combustion.

The primary objective of this work is to improve understanding of combustion dynamics through an experimental study of lean premixed combustion using a low swirl combustor. The major effect of con-finement is shown to be a change in flame structure in both the forced and unforced cases. This effect is captured using the parameter $L_{f,CoHR}/D_{comb}$, which describes the changing degree of flame–wall interaction in each combustor size. The measured FTF data, as a function of confinement, are then generalized by Strouhal number. Data from the two larger combustors are collapsed by multiplying the Strouhal number by the confinement ratio to account for the flow expansion ratio and change in convective velocity within the combustor. Trends at the transfer function extrema are also assessed by examining them in the context of confinement and by using flame images. A change in the fluctuating structure of the flame is also seen to result from an increase in confinement.

Introduction:

The current generation of lean-premixed gas turbines used for power generation are susceptible to large thermoacoustic instabil-ities as a consequence of their design and operation. These insta-bilities are governed by a feedback process between heat release rate fluctuations, acoustic pressure fluctuations, and fluctuations in mixture composition entering the combustion chamber. Unstable combustion is undesirable in gas turbine systems as it leads to reduced efficiency and can eventually lead to severe system damage [1,2].Due to the problems caused by combustion instability, there is currently significant industrial interest in understanding the gov-erning physics of combustion instabilities and developing physics-based models to aid in the design of practical

ISSN No: 2348-4845
International Journal & Magazine of Engineering, Technology, Management and Research
A Peer Reviewed Open Access International Journal

gas turbine devices [3]. Predictive models used in the design stage of gas tur-bine manufacture require an analytical or numerical model of the flame's response to inlet perturbations. The FTF, introduced by Merk [4], is a construct that is used to describe flame response in these models and can be determined experimentally. The FTF describes the heat release response of the flame to a given input perturbation. In the fully premixed mode of operation considered in the present study, the FTF, as shown in Eq. (1), is used to relate

the normalized inlet mixture velocity fluctuation u = 0 u_ ð Þ to the nor-malized heat release rate fluctuation ðQ-0 =Q- Þ produced by the flame at a given frequency of modulation ðxÞ.

FTFðxÞ ¼ Q-0 =Q- / u0=u_ (1)

An investigation into the effect of lateral confinement (combus-tor diameter) on a premixed, bluff body stabilized laminar flame was performed by Birbaud et al. [18,19]. The combustor diameter was varied and shown to have a "significant effect" on the dynam-ics of the flame. The reduction in flame tip motion caused by the flame–wall interaction and a modification of the flame–vortex interaction process was cited as the cause of this change; in the presence of the wall, the mechanism of vortex roll-up [7]. Numerous mechanisms that link velocity fluctuations within a system to heat release rate fluctuations have been proposed in the literature [5,6]. In turbulent, fully premixed flames, acoustic fluc-tuations in mixture velocity have been shown to result in vortex production [7,8], swirl fluctuations [9,10], and helical disturbances [11]. These disturbances all produce perturbations in flame area, resulting in fluctuations in the heat release rate from the flame. While there has been a significant amount of research com-pleted in the field of gas turbine combustion instability, much of this work has been completed using test facilities that are simpli-fied relative to practical devices, typically by considering only a single flame under constant confinement. These studies have been useful in developing an understanding of the mechanisms control-ling combustion instability [2,8], but more complex experiments have shown that significant differences exist between the response of these simplified systems and more realistic multiple-flame con-figurations [3,12–15]. In particular, each flame in a multiflame combustion system experiences varying confinement and interac-tion with adjacent flames within the combustor.

The additional complexity of varying confinement is not considered in the major-ity of single-nozzle experiment and is, in part, responsible for the differences in the flame response of single and multiflame devices [13,14,16,17]. was altered such that a new mechanism of "flame tip folding" was found to be the dominant process driving flame area fluctuations. Cuquel et al. also studied the effect of confinement on laminar flames [20].

The response of the conical flames studied was gener-alized using aconfinement ratio (the ratio of injector to combustor diameter) and burnt to unburnt gas expansion ratio. These parameters were used to account for the difference in convective velocity and pressure in the combustor due to flow expansion and the combustion process. The effect of varying confinement on a turbulent, nonreacting flow field was considered by Fu et al. in a study of various rectan-gular ducts using laser Doppler velocimetry [21]. The width of the duct was found to have an effect on the flow field shape and struc-ture. Various profiles within the flow changed with the duct size, including the size and strength of the central and corner recircula-tion zones and the corresponding shear layer locations. In addi-tion, a transition between different flow regimes (described as similar to wall-jet and free-jet regimes) was found to occur at a critical value of confinement.

ISSN No: 2348-4845
International Journal & Magazine of Engineering, Technology, Management and Research
A Peer Reviewed Open Access International Journal

A similar result was shown by Fanaca et al. [14], who found that this transition between flow fields of different types affected the response of the flame in an annular configuration. The effect of confinement in the turbulent case was further tested by Hauser et al. [16], who reported data for both a highly confined and less confined swirl-stabilized flame in a square combustor. A difference in the FTF in each case was noted and attributed to changes in the time delays associated with the change in flame shape in each confinement. It was hypothe-sized that flames in the more confined case had reduced gain due to a reduction in phase delay caused by the increased flow rate through the combustor.Previously completed research in the area of flame–wall inter-actions provides useful insight into the mechanisms governing flame response as the confinement is changed. A problem arises, however, as the majority of this work represents cases which are unrealistic in terms of actual gas turbine combustion. For exam-ple, the early work performed by Birbaud et al. [18,19] investi-gated laminar flames and the work of Fu et al. [21] concerned nonreacting flow fields.

While some experimental data in turbulent systems have been provided by other authors (i.e., Hauser et al. [16] and Fanaca et al. [14]), the range of conditions assessed in each study was limited and attempts were not made to generalize the results across a broad range of conditions or combustor sizes. Further work is, therefore, required to assess the impact of lat-eral confinement on gas turbine flame response. This paper addresses this issue and details an investigation into the effect of combustor diameter on the FTF response of a turbulent, fully pre-mixed, swirl-stabilized combustion system. Particular efforts are made to generalize the effect of confinement across a wide range of operating conditions in order to assess consistent trends and mechanisms governing the response of the flame in each case.The effect of the thermal boundary condition at the combustor wall on flame response was investigated in models developed by Tay-Wo-Chong and Polifke [22] and Kedia et al. [23].

In each case, the flame geometry was found to change as the wall heat flux was altered. Specifically, flame stability was improved as the heat losses from the flame were reduced. This work also high-lighted the critical link between flame structure and response, an effect that has been well described in the literature [24,25].

Experimental Configuration and Method:

Measurements are obtained using an industrially designed lean-premixed, swirl-stabilized, single-nozzle combustor. The combus-tion chamber is open to the atmosphere such that all tests are com-pleted at atmospheric pressure. The major components of thesystem are: an air heater, siren, inlet manifold, swirl-stabilized in-jector, and an optically accessible combustion chamber. High-pressure air enters the test facility at a rate of up to 0.35 kg/s at2 MPaThe air is then heated in a 50 kW process air heater. In thefully premixed mode of operation studied here, natural gas fuel(>95% methane) is injected upstream of a choked orifice into thepreheated air.

The orifice prevents pressure oscillations in thedownstream sections from affecting the fuel flow rate and alteringthe mixture composition during operation. The fuel injection loca-tion is far upstream of the combustor to allow for complete mixingbefore combustion occurs. Before entering the injector, part of the fuel–air mixture passes through a rotor/stator siren device used to impose velocity oscillations upon the flow field. The flow then enters the inlet section and passes through the injector illustrated in Fig. 1 (swirl number _0.7). The flame is confined by a fused-silica quartz combustor (type GE 214), which provides optical access to the flame.The degree of lateral confinement and, therefore, flame–wall interaction, is varied using three combustors of different diame-ters. Each combustor is clamped onto the dump plane using a con-finement ring which serves to both concentrically locate the combustor and provide cooling air to its outer surface (see Fig. 1).

ISSN No: 2348-4845
International Journal & Magazine of Engineering, Technology, Management and Research
A Peer Reviewed Open Access International Journal

The combustors used in this study are 0.11 m, 0.15 m, and 0.19 m in diameter with a length of 0.305 m and a wall thickness of 0.005 m. The resulting confinement ratios (C_r) are 0.5, 0.37, and 0.29 when calculated using the diameter of the nozzle relative to the combustor diameter. Figure 2 shows projection (line-of-sight), time-averaged, CH* chemiluminescence intensity images for the three combustor diameters used in this study. The direction of flow is from left to right for these and all other figures in this pa-per. The colorbar indicates the chemiluminescence intensity which is linearly proportional to heat release rate for fully pre-mixed flames [26,27]. Black corresponds to zero intensity while white corresponds to the maximum intensity within a particular image. The degree of flame–wall interaction is different in each combustor as evidenced by the change in flame structure and spreading of the flame along the combustor wall. The dark region at the base of each image is a result of the confinement ring sys-tem used to clamp the combustors in place as it obscures the bot-tom 0.013 m of each image.

The range of operating conditions investigated in this study is shown in Table 1. Conditions were chosen to match the flow fac-tor of the industrial injector and to operate in the lean-premixed mode of combustion. The forcing frequency range was chosen based on past research showing that flames act as low-pass filters and that the gain is reduced at increased frequencies [28]. All test-ing was performed using a 5% forcing amplitude (root-mean-square of the mean velocity) such that the flame response is expected to be in the linear regime [29–31]. Fifty-four independ-ent transfer functions were measured.Static pressure fluctuations are measured at two locations in the injector using piezoelectric pressure transducers (PCB model 112A22). In conjunction with the two-microphone method [32,33], these signals are used to determine the fluctuating veloc-ity within the injector. In order to characterize the global heat release rate from the flame, a photomultiplier tube is used to re-cord the chemiluminescence emitted during the combustion pro-cess. A narrow bandpass filter is used to collect the chemi-luminescent light emitted at 432 6 5 nm, corresponding to emission from CH* and CO^*_2 radical species. The effect of wall temperature on chemi-luminescence was assessed by varying the

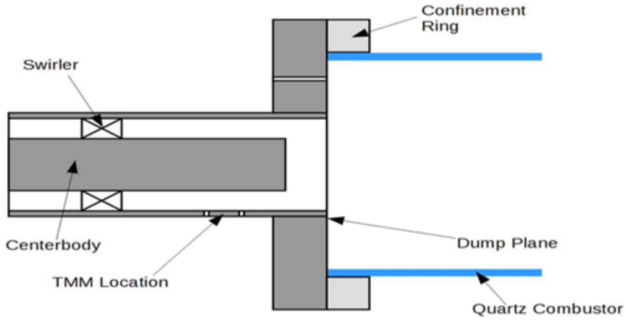

Fig. 1 Test section geometry

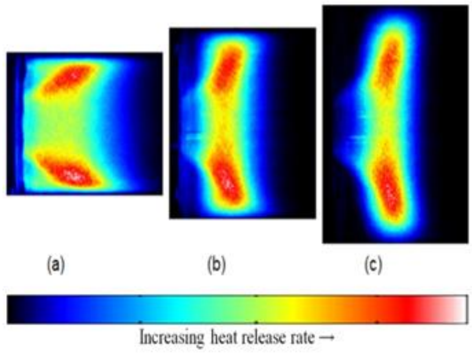

Fig. 2 Comparison of projection flame images in three differ-ent diameter combustors (images hown to scale): (a) 0.11 m, (b) 0.15 m, and (c) 0.19 m

cooling provided to the combustor by the confinement ring. Over the range of combustor wall temperatures assessed (423–873 K at the flame center of heat release (CoHR) location), no change was found in the measured chemiluminescence signal or the flame structure and response to instability. All data acquisition and mea-surement systems are controlled using a National Instruments LAB-VIEW system coupled with a data acquisition board (model 6259). The data are recorded for 32 s at each test condition with a sam-pling rate of 8192 Hz. The recorded time-series signals are then converted into the frequency domain using a fast Fourier trans-form to provide information about the fluctuations at the frequen-cies of interest.

ISSN No: 2348-4845
International Journal & Magazine of Engineering, Technology, Management and Research
A Peer Reviewed Open Access International Journal

A high-speed camera (Photron SA-4) coupled with an image intensifier (Invisible Vision UVi 1850-10) and a bandpass filter (432 65 nm) is used to image the flame. Four thousand images are acquired at a rate of 4000 frames per second using an exposure time of 200 ls in order to accurately resolve the time-varying flame structure. The camera resolution is _0.45 mm per pixel for all reported data. These images are used to determine the time-averaged flame structure and phase-averaged variation in structure and heat release rate at any operating condition [9,15]. As the camera captures integrated line-of-sight (projection) images, an inverse Abel transform is applied to deconvolute the images.

This process yields emission images which represent a two-dimensional slice of the flame [34,35]. These emission images are then radially (r) weighted to account for the increase in flame area with radius. An example of each of these different images is given in Fig. 3. All measured flames were axisymmetric; therefore, only the top-half of each image is shown. The injector geometry and combustor wall are indicated in solid gray.Several measurements of flame structure can be calculatedbased on the flame images. The flame length ($L_{f,CoHR}$) is measured from the centerbody edge where the flame is anchored to the area-weighted location of maximum intensity within the image, also referred to as the flame's CoHR [36]. This length represents the distance that a perturbation originating at the flame base has to travel before interacting with the region of highest heat releaserate within the flame. $L_{f,CoHR}$ also relates to the phase delay between the inlet velocity perturbations and resulting heat releaserate oscillations.

Table 1 Range of operating conditions

Parameter	Range
Inlet velocity (m/s)	20–35
Inlet temperature (K)	373–523
Equivalence ratio (U)	0.55–0.70
Forcing frequency (Hz)	100–450
Forcing amplitude (%)	5
Combustor diameter (m)	0.11, 0.15, 0.19
Combustor length (m)	0.305

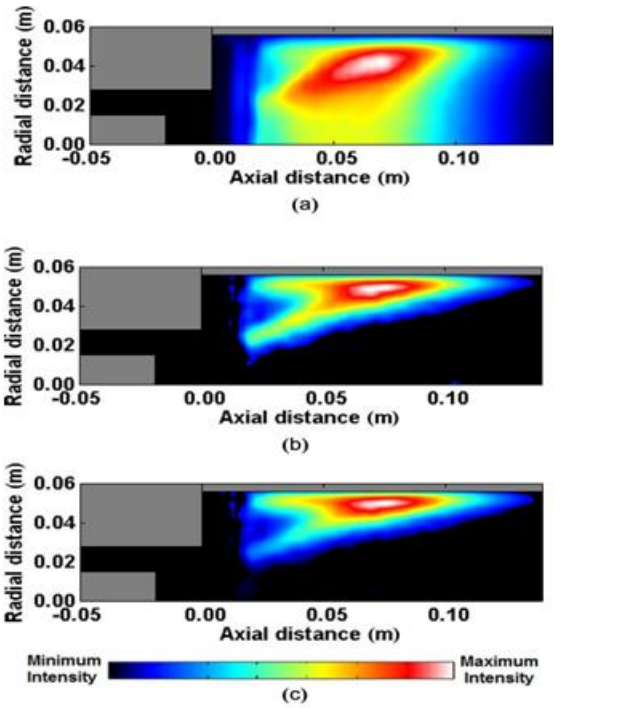

Fig. 3 Illustration of the image processing procedure: (a) pro-jection (line-of-sight) image, (b) emission image (deconvoluted projection image), and (c) revolved image (r-weighted emission image). Operating condition: 25 m/s inlet velocity, 5% forcing, 473 K preheat, and U50.6 in the 0.11 m diameter combustor

If the intensity within the image is summed in the radial (verti-cal) direction, an axial heat release rate profile (AHR) results (Fig. 4). This profile gives an indication of the distribution of the recorded heat release from the flame along the axis of the combus-tor. The full width at half-maximum (FWHM) of this profile is also shown in Fig. 4. This value is calculated by finding the width of the peak in the axial profile at an intensity value of half of the peak value.

ISSN No: 2348-4845
International Journal & Magazine of Engineering, Technology, Management and Research
A Peer Reviewed Open Access International Journal

The FWHM is representative of the axial distribution of the flame's heat release [37]; it is a single value which allows for comparisons of this distribution between different operating conditions to be made.In addition to calculating these image metrics, the high-speed image set is also processed to examine the fluctuating behavior ofthe flame. For the time-series data captured by the high-speed camera, a Fourier transform is used to resolve the mean behavior, and information about the fluctuations (RMS amplitude and phase) at the frequencies of interest.

The spatially resolved heat release fluctuations within a sample flame are shown in Fig. 5 in terms of the "heat release rate index" (analogous to the Rayleigh index [38]). The heat release rate index is calculated by correlating the heat release rate fluctuation at each pixel with the fluctuation in the global heat release rate over a forcing cycle. This image gives an indication of the contribution of each region in the flame to the global response of the flame in terms of both amplitude and phase. A hot–cold color scale is used for the heat release rate index image. Hot colors represent areas that are in phase with the global fluctuation in heat release rate and that have high amplitude fluctuations.

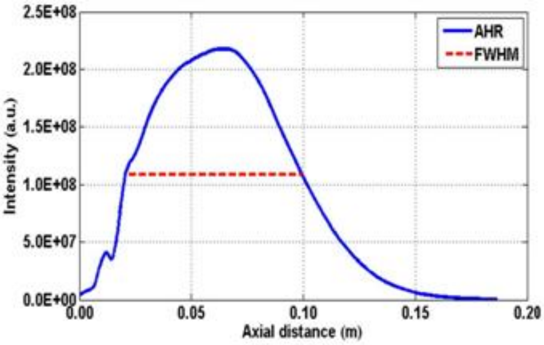

Fig. 4 Axial heat release profile (AHR), FWHM measurement overlaid. Operating condition: 25 m/s inlet velocity, 5% forcing, 473 K preheat, and U50

Cool colors show the opposite effect; areas that are of varying magnitude but out-of-phase with the global flame response. For the flame shown in Fig. 5, the global heat release rate perturbation is driven by a large fluctuation in heat release rate in the downstream region of the flame (the large orange region) that is in phase with the global response.

Results and Discussion:

Figure 6 shows the images of unforced, time-averaged, revolved flame in the three combustors investigated. The operat-ing condition is identical for each flame. The change in the degree of wall interaction and its effect on the stable flame structure can clearly be seen in the images. Figure 6(a) shows the stable flame structure in the smallest, 0.11 m diameter combustor. Here, the flame impinges upon the wall and spreads in both the upstream and downstream directions. The degree to which the flame is "flattened" in the near-wall region can be viewed as a measure of the strength of the flame–wall interaction. The flattening of the flame by the wall decreases as confinement is reduced, as visibly demonstrated in Figs. 6(b) and 6(c).

The location and extent of the FWHM is overlaid in white along the lower edge of each image and appears to be a good approximation of the changing heat release distribution as confinement varies.he flame structure in the 0.11 m diameter combustor (Fig. 6(a)) is significantly different than the structure in the larg-est, 0.19 m diameter combustor (Fig. 6(c)) where there is little evi-dence of an interaction between the flame and the wall. In the largest combustor, the flame's heat release is concentrated in a smaller region 0.06 m downstream of the dump plane, and the smaller FWHM captures the corresponding decrease in heat release rate distribution.

The 0.15 m diameter combustor repre-sents a condition between these two extremes with a moderate degree of flame–wall interaction and some degree of flame spread-ing. Figure 6, therefore, indicates that confinement has a strong impact on the axial distribution of the heat release rate within the flame. Flames in the larger combustors also show a greater degree of curvature than those in 0.11 m diameter case.

ISSN No: 2348-4845
International Journal & Magazine of Engineering, Technology, Management and Research
A Peer Reviewed Open Access International Journal

This change is in-dicative of a change in the flow field within the combustor and is perhaps related to the jet profile (i.e., free- or wall-jet) as it exits the nozzle.Although the extent to which the flame interacts with the wall changes with operating condition, the flame images shown in Fig. 6 can be viewed as typical of the time-averaged, unforced flame structure in each combustor over the range of conditions tested. In the smallest combustor, the flame always interacts strongly with the confining boundary, while in the 0.19 m diameter combustor, there is very little evidence of an interaction with the confinement.Figure 7 describes the values of various flame metrics under variable confinement. The flame CoHR location is plotted in Fig. 7(a) in terms of x- and y-coordinates relative to the center-body edge at the axis origins. In the tightest confinement, the CoHR is located along the combustor wall in all cases. This con-trasts flames in the larger, 0.15 m and 0.19 m diameter combustors which show a wider variation in CoHR location and flames that exist further away from the combustor wall.The ratio of flame length to combustor diameter ($L_{f,CoHR}/D_{comb}$) has been used in previous studies in order to nondimensionalize flame response behavior [1,39,40]. This ratio has physical signifi-cance in that it approximates the flame base angle and aspect ratio, factors known to be controlling parameters in flame response [8,20,25,41]. For this reason, the parameter $L_{f,CoHR}/D_{comb}$ has been used in generalizing FTFs [39]. It is used here as a measure

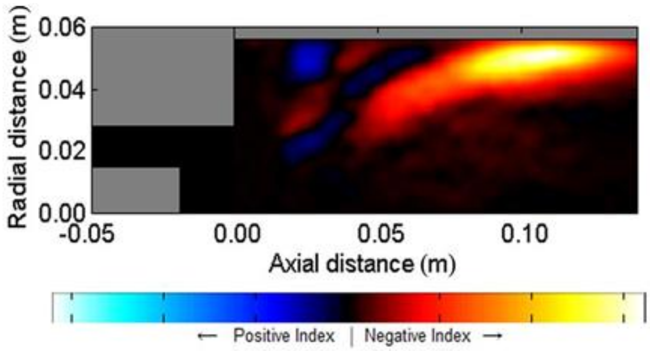

Fig. 5 Example heat release rate index image. Operating con-dition: 25 m/s inlet velocity, 5% forcing, 473 K preheat, and U 50.6 in the 0.11 m diameter combustor at 120 Hz modulation.

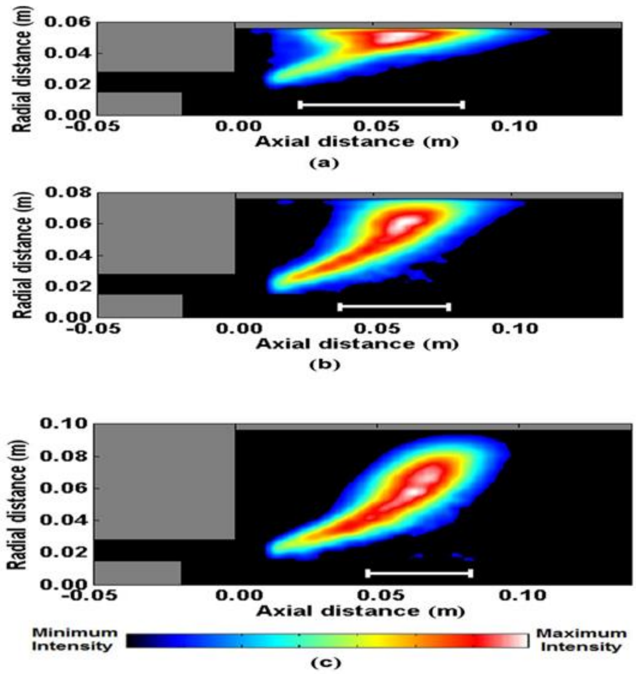

Fig. 6 Time-averaged, radially weighted, deconvoluted chemi-luminescence flame structure comparison for three combustor sizes: (a) 0.11 m diameter combustor, (b) 0.15 m diameter combustor, and (c) 0.19 m diameter combustor. Operating con-dition: 22.5 m/s inlet velocity, 5% forcing, 473 K preheat, and U 50.65.

of the degree of confinement, to which its suitability is demon-strated in Figs. 7(b) and 7(c). For a given combustor diameter, it is expected that as the flame length increases, the degree of wall interaction will also increase as the flame must eventually impinge on the wall, a statement evidenced by the behavior of the flame in the smallest combustor in Fig. 7(a).Figure 6 indicates that the FWHM could be used to describe the degree of flame spreading caused by confinement. This hypothesis is tested in Fig. 7(b) which shows the FWHM plotted against$L_{f,CoHR}/D_{comb}$. The data reveal a trend in that the FWHM increases with increasing $L_{f,CoHR}/D_{comb}$ in each individual confinement case and across all confinements in general. In the 0.11 m diameter case, the FWHM increases more rapidly withincreasing $L_{f,CoHR}/D_{comb}$ than in the less confined cases.

ISSN No: 2348-4845
International Journal & Magazine of Engineering, Technology, Management and Research
A Peer Reviewed Open Access International Journal

A degree of overlap between flames in the 0.15 m diameter combustor withthose in both larger and smaller confinement is evidenced and shows the range of flame spreading that is achievable in this caseby changing operating conditions. Both the FWHM and $L_{f,CoHR}$/ D_{comb} parameter are shown to be suitable measures of the degreeof flame–wall interaction.Figure 7(c) details the percentage of the total heat release from the flame that is located within 0.01 m of the combustor wall plot-ted against $L_{f,CoHR}/D_{comb}$. In the tightest confinement (0.11 m di-ameter), approximately 60% of the total heat release from theflame is located in this region. The percentage of the total image intensity near the wall reduces with increasing combustor size such that cases in the largest combustor exist with only 10% of their total intensity in the near-wall region. Again there is evi-dence of some overlap in the data of the 0.15 m diameter combus-tor with the 0.19 m diameter case. It is clear from these data that the confinement also has a strong impact on the radial distribution of the flame's heat release, in addition to altering the spread of the flame's heat release axially. The strong, positive trend in the datawhen plotted against $L_{f,CoHR}/D_{comb}$ again indicates that this pa-rameter is appropriate for use in describing the degree of wallinteraction in the various cases considered in this study; both Figs. 7(b) and 7(c) show that for cases with stronger degree of flame–wall interaction, the numerical value of $L_{f,CoHR}/D_{comb}$ is increased.

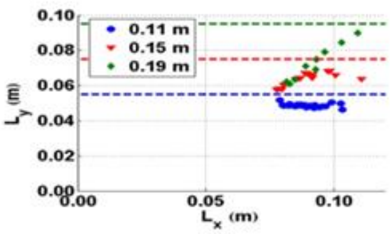

(a)

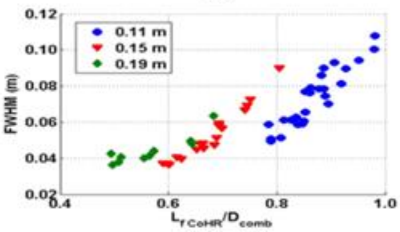

(b)

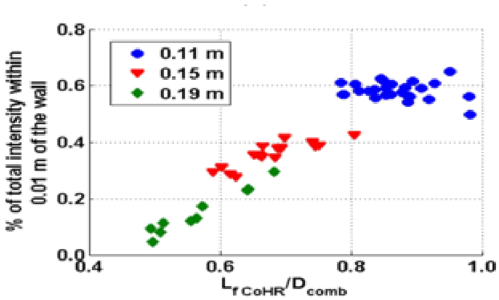

(c)

Fig. 7 Flame structure parameters under variable confine-ment. (a) Flame CoHR coordinates. The location of the combus-tor wall is indicated by the dashed lines. (b) FWHM plotted against flame length/combustor diameter. (c) Percentage of total heat release in the near-wall region as a function of the flame length divided by combustor diameter.

While the overall trends shown in Fig. 7 are consistent across all combustor sizes, there is a suggestion that the behavior of the flame changes somewhat for values of $L_{f,CoHR}/D_{comb}$ greater than 0.8 (in the most confined case); in Figs. 7(b) and 7(c), there is a positive slope and the y-axis values increase with $L_{f,CoHR}/D_{comb}$ in all cases. The data from the 0.15 m and 0.19 m diameter confine-ment show some degree of overlap but the same cannot be said for the 0.11 m diameter combustor data. The measurements from this confinement do not overlap the other data, and in Fig. 7(c) in particular, there appears to be a change in the trend of the data in the 0.11 m confinement relative to the other sizes.

While there is not enough evidence to fully describe this change, the lack of overlap in the 0.11 m diameter case could relate to the phenomena discussed by Fu et al. [21] and Fanaca et al. [14] who found that the flow transitioned from a free-jet to a wall-jet at a certain value of confinement. Such a change is consistent with the images shown in Fig. 6 and the data presented in Fig. 7. Figure 8 shows measured transfer function data for flames in the three different combustor sizes at the same operating condi-tion.

ISSN No: 2348-4845
International Journal & Magazine of Engineering, Technology, Management and Research
A Peer Reviewed Open Access International Journal

Differences in both the gain and phase of the measured data are seen to result from the change in confinement. The magnitude of the gain at a given frequency changes with combustor diameter. In addition, the frequencies corresponding to the FTF maxima and minima shift with confinement. The reduction in gain in the small-est combustor at higher frequencies (above the gain minimum) relative to the other two confinement cases is consistent through-out this study.Comparing the phase data between the three cases, the slope of the phase varies from approximately _5 deg/Hz in the smallest combustor to _3 deg/Hz in the other combustor sizes. The location of the inflection point in the phase also varies with confinement and is linked to the frequency of the gain minimum condition in each case.The trend of alternating minima/maxima and the linear phase behavior observed in Fig. 8 is typical of transfer function data reported in the literature [2,8,10]. For example, in the 0.11 m di-ameter case in Fig. 8, there is an initial high gain condition at 120 Hz followed by gain minimum at 200 Hz and another maxi-mum at 340 Hz. These conditions are important as they represent locations at which the multiple mechanisms governing flame response are either constructively or destructively interfering [6]. The behavior of the flame at these maxima and minima is exam-ined further in Figs. 11–14.

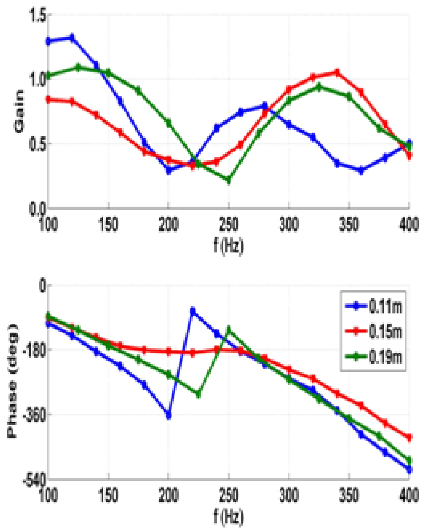

Fig. 8 Transfer function gain and phase data for the three dif-ference combustor sizes. Operating condition: 22.5 m/s inlet velocity, 5% forcing, 473 K preheat, and U50.65.

Data for all 54 transfer functions measured in this study are plotted in Fig. 9. The lack of a consistent trend in the data is expected. Previous studies have noted that although transfer func-tions at different operating points appear qualitatively similar, normalization parameters are required to collapse the data [17,36,42]. An example of a parameter often used to do this is the Strouhal number (Eq. (2)), defined as the ratio of the forcing fre-quency ($f_{forcing}$) multiplied by flame length ($L_{f,CoHR}$) to the inlet velocity in the nozzle (V_{inlet}). This ratio describes the wavelength of the convective perturbation driving flame response relative to the flame length and has been shown to be a controlling factor in laminar flame response [25,28].

$$S_t = \frac{L_{f;CoHR} \, f_{forcing}}{V_{inlet}} \qquad (2)$$

Figure 10 shows the measured FTF data for all 54 operating conditions plotted against the Strouhal number. Qualitatively, a collapse in the data is achieved along the horizontal axis and some general trends in the data are revealed. In particular, the response of all flames at low values of Strouhal number is similar. For all conditions, there is a peak in the gain at a Strouhal number of approximately 0.5. The FTF gain at all operating conditions and confinements is also minimized around a Strouhal number of unity, although the collapse is imperfect. A difference in the

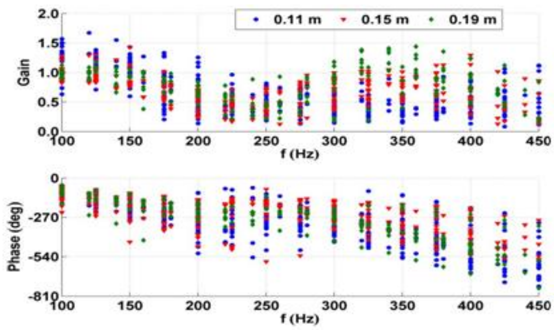

Fig. 9 Measured transfer function data for all test conditions

ISSN No: 2348-4845
International Journal & Magazine of Engineering, Technology, Management and Research
A Peer Reviewed Open Access International Journal

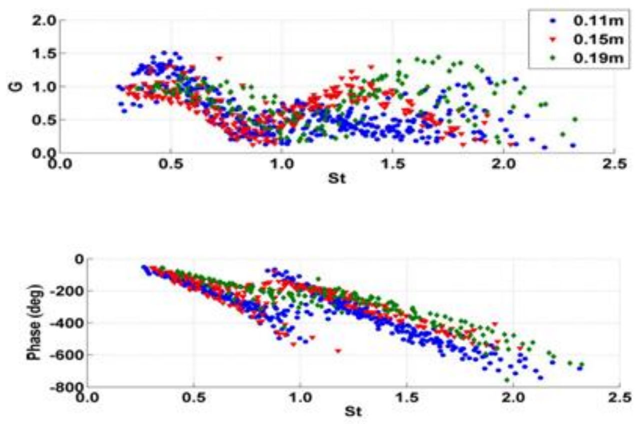

Fig. 10 Collated flame transfer function gain and phase nor-malized by Strouhal number

general trend of the transfer function gain is seen for each of the different combustor sizes at higher values of Strouhal number. For example, the gain of flames in the smallest combustor remains rel-atively low at high Strouhal numbers (high frequencies), while the gain of flames in the less confined cases rises to values above unity. This difference in response is most pronounced in the larg-est combustor which shows a peak in the transfer function gain around a value of St ¼ 1.5–1.8, with gain values of one or higher. In general, there is a clear effect of combustor diameter on the transfer function gain response; as confinement increases, the gain at high frequency is reduced.

In all confinement cases plotted in Fig. 10, the behavior of the phase is similar. An inflection point exists for all cases around St _ 0.8, the gain minimum condition. There is also a deviation in the slope of the phase at high frequency which is consistent with combustor diameter. The phase of the transfer function in the 0.11 m diameter case decreases more quickly than the other two cases, indicative of a reduced time delay in this case. This change in the time delay is likely to be indicative of the structural changes in the flame that result from confinement in addition to the chang-ing expansion ratio in each case as the flow enters the combustor.The overall degree of collapse in the transfer function gain with Strouhal number is suggestive of the impact of convective distur-bances upon the flame. The peak in the data at a Strouhal number of _0.5 and the gain minimum occurring at St _ 1.0 is a strong in-dication that the ratio of the flame length to the perturbationwave-length is an important factor in determining low-frequency flame response when the flame is convectively compact. Above St ¼ 1.0, larger differences in the response of each flame with confinement arise and the Strouhal number is less effective at collapsing the data. This is an indication that as the flame becomes noncompact to disturbances (convective wavelength < flame length), the effect of confinement becomes more pronounced and results in a change in FTF behavior.Figure 10 demonstrates that at the extrema in the transfer func-tion gain, the general behavior of the flame in each confinement is slightly different. Figure 11 highlights this behavior by plotting the gain at these conditions against the confinement parameter$L_{f,CoHR}/D_{comb}$. Figure 11(a) shows that the gain at the initial, low-frequency peak (at St _ 0.5) is positively correlated with $L_{f,CoHR}/D_{comb}$. As confinement increases, the initial gain maximum increases in amplitude. This result extends previously reported results discussed as a function of this parameter [1] to turbulent flames under variable confinement. The gain of the second FTF maximum (found at high frequen-cies or Strouhal numbers above unity) is plotted in Fig. 11(b). In this case, the gain magnitude decreases with increasing

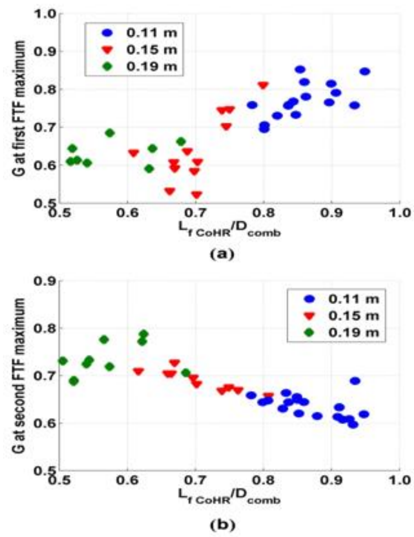

ISSN No: 2348-4845
International Journal & Magazine of Engineering, Technology, Management and Research
A Peer Reviewed Open Access International Journal

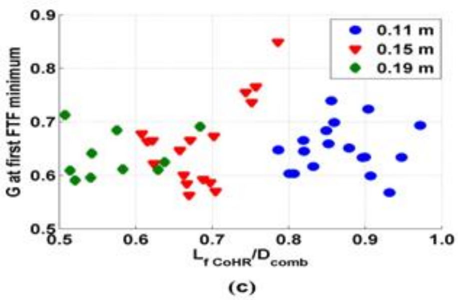

Fig. 11 Trends in FTF extrema with the flame length/combus-tor diameter parameter: (a) initial gain maximum, (b) second gain maximum, and (c) first gain minimum

confinement, a trend that is counter to the relationship exhibited at the first gain maximum (Fig. 11(a)). The change in the sign of the correlation indicates a change in the role of the mechanism gov-erning flame response. While the $L_{f,CoHR}/D_{comb}$ parameter cap-tures the trends at both the gain maxima in the FTF data, the change in the nature of the trend (positive to negative) precludesthe use of $L_{f,CoHR}/D_{comb}$ in normalizing FTF gain data (i.e., Fig. 10 vertical axis) over the range of conditions studied here. A gen- eralization of FTF gain data using $L_{f,CoHR}/D_{comb}$ has been

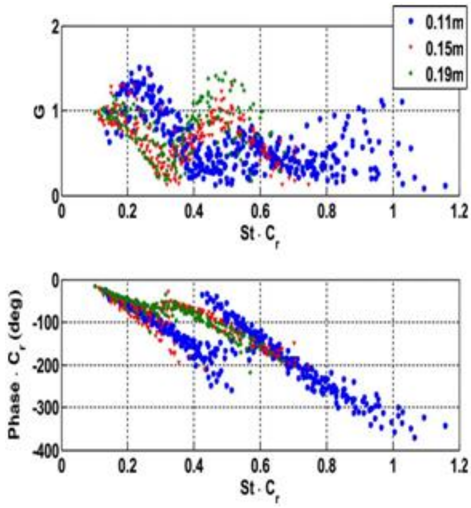

Fig. 12 Collated FTF gain and phase normalized by Strouhal number multiplied by confinement ratio

attempted previously, although only for cases with a single FTF maximum [36].

The data shown here indicate that when multipleextrema exist within the FTF, the $L_{f,CoHR}/D_{comb}$ parameter may not collapse the measured data. The change in the sign of the trends in Figs. 11(a) and 11(b) is perhaps related to the Strouhal number effect in that at the first gain maximum, the flame is convectively compact and gain increases with flame length as the wavelength of the disturbance is very large relative to the flame. At the second maximum, how-ever, there are multiple perturbations present within the flame. The gain magnitude is, therefore, reduced as the flame length is long relative to the perturbation wavelength and there are multiple positive and negative fluctuations present within the flame at any instant.

Figure 11(c) shows no correlation between the confinement pa-rameter, $L_{f,CoHR}/D_{comb,}$ and the gain magnitude at the minimum gain frequency. This indicates that the controlling mechanism governing flame dynamics is different than at the high magnitude gain cases. $L_{f,CoHR}/D_{comb}$ effectively generalized other effects of confinement; therefore, the lack of correlation here demonstratesthat the physical processes which govern the gain minimum con-dition are independent of the degree of flame–wall interaction. Figure 12 shows collated FTF data with the horizontal axis nor-malized by the product of the Strouhal number (St) and confine-ment ratio (C_r).

This product not only introduces the ratio $L_{f,CoHR}/ D_{comb}$ into the horizontal axis normalization but also accounts for the expansion of the flow from the injector into the combustor and the change in convective velocity caused by this expansion. The vertical phase axis is also normalized by the confinement ratio (C_r). Again, using the confinement ratio accounts for the change in convective velocity and, therefore, phase delay when the combustor diameter is varied. Plotting the FTF gain and phase against the product of Strouhal number and confinement ratio generalizes the data from the 0.15 m and 0.19 m diameter combustors.

ISSN No: 2348-4845
International Journal & Magazine of Engineering, Technology, Management and Research
A Peer Reviewed Open Access International Journal

The location of the max-ima and minima in the gain is shifted such that they occur at simi-lar x-axis values and the curves overlap. This collapse is in contrast to Fig. 10, in which the Strouhal number alone cannot collapse the gain data between confinements. The phase data for the two larger combustor cases are similarly collapsed with the location of the inflection point occurring at the same value of St C_r. This collapse is extremely important as it shows that the mech-anisms governing flame response in each case are the same and also allows for predictions of flame response to be made. The data from the 0.11 m diameter combustor are not collapsed by multiplying the Strouhal number with confinement ratio. This lack of collapse is indicative of the confinement ratio not captur-ing the important physical mechanisms that affect the response of the flame in this case.

If the confinement ratio is taken to beindicative of the expansion ratio, this lack of collapse could be related to a change in flow regime from a free-jet to a wall-jet in the smallest combustor. Such a change has been noted in prior studies of confinement and would lead to a lesser dependence on the flow expansion ratio as the velocity no longer decays through the expansion of the flow area; it decays due to an interaction with the combustor wall which is not described by C_r. This hypothesis is further reinforced by the data plotted in Figs. 6 and 7, which highlight the change in flame structure and strength of flame–wall interaction with confinement.

The lack of collapse in the transfer function data plotted in Figs. 10 and 12, along with the differences in behavior at the gain maxima shown in Fig. 11, is investigated using flame images in Fig. 13. This figure shows heat release rate index images which correlate the spatial distribution of the fluctuating heat release of the flame with the global heat release response. Each image is self-scaled. The figures plotted are shown for the same operating condition and at the second gain maximum condition, which cor-responds to 300 Hz for the most confined (0.11 m diameter) case and 350 Hz for the less confined (0.15 m and 0.19 m diameter) cases. Approximately one-and-a-half perturbation wavelengths are present in the flame in each case, indicated by the alternating pockets of in-phase and out-of-phase fluctuations starting at the centerbody and ending along the combustor wall.

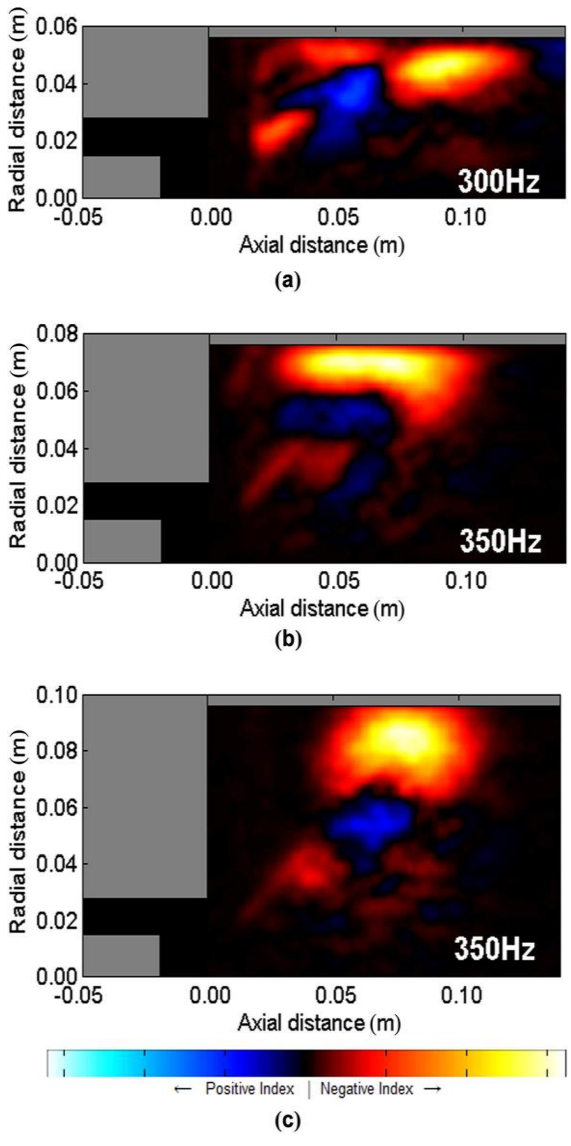

Fig. 13 Heat release rate index images for the second gain maximum condition: (a) 0.11 m diameter combustor, (b) 0.15 m diameter combustor, and (c) 0.19 m diameter combustor. Oper-ating condition: 25 m/s inlet velocity, 5% forcing, 473 K preheat, and U50.6.

ISSN No: 2348-4845
International Journal & Magazine of Engineering, Technology, Management and Research
A Peer Reviewed Open Access International Journal

The number of perturbations within the flame is expected to roughly indicate the global response (or gain) of the flame, based on a simple length scale analysis. For example, a single-half per-turbation present in the flame should result in a gain maximum, while a full perturbation should result in a gain minimum, as the response in one part of the flame cancels the response of another part of the flame. Given that 1.5 perturbations are present in Fig. 13, the Strouhal number of each image is expected to be 1.5. Figure 10, however, indicates that this is not the case and that the approximate Strouhal number calculated using Eq. (2) is inaccu-rate, likely due to the approximations made by using the flame lengt
h and mean inlet velocity in the calculation. The reduced fre-quency at which the same behavior is seen in the 0.11 m diameter combustor, compared to the larger case, suggests that the flame in the smallest combustor becomes convectively noncompact at a lower frequency than flames in the larger combustors.

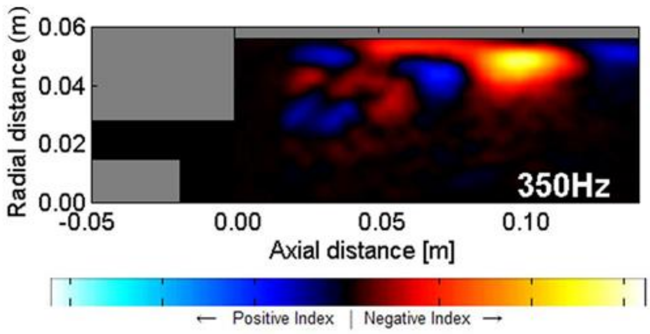

Fig. 14 Heat release rate index image for a flame in the 0.11 m diameter combustor at 350 Hz. Operating condition: 25 m/s inlet velocity, 5% forcing, 473 K preheat, and U50.6

The images shown in Fig. 13 also indicate a change in the fluc-tuating structure of the flame, particularly in the smallest combus-tor relative to the other sizes. In Figs. 13(b) and 13(c), the heat release rate fluctuation is dominated by a single large fluctuation at the flame tip (bright orange in each case). In the 0.11 m diame-ter case (Fig. 13(a)), however, the fluctuation at the flame tip is split into two regions.

A smaller high-intensity region of heat release fluctuations exists in the downstream region of the flame while other fluctuations exist along the combustor wall and close to the recirculation zones. This change in the fluctuating structure of the flame relative to the 0.15 m and 0.19 m diameter cases is perhaps responsible for the lack of collapse when data from this combustor are plotted against St C_r. The behavior of the flame under excitation is different and is likely to be scaled by a differ-ent parameter.

Figure 14 shows the heat release rate index image from the smallest combustor at the same operating condition and forcing frequency (350 Hz) as the flames shown in Figs. 13(b) and 13(c). The gain of the flame in Fig. 14 is no longer a local maximum, but now lies between a local maximum and minimum. Approxi-mately two complete wavelengths, evidenced by four alternating regions of in-phase and out-of-phase heat release, are now visible in the flame instead of the one-and-a-half wavelengths present at 300 Hz (Fig. 13(a)). Comparing this image to images of the other confinement cases at 350 Hz (Figs. 13(b) and 13(c)) indicates that the flame in the smallest combustor becomes convectively non-compact at a lower frequency than the flames in the larger con-finement cases.

Figures 10 and 12 also showed this effect in that the collapse between all combustor diameters was imperfect. If FTF behavior is assumed to be generalized by Strouhal number (modified or not), this disagreement with changing confinement indicates that the effective length of a turbulent, wall-interacting flame is not completely captured by $L_{f,CoHR}$. Figure 14 suggests that the actual flame length in the 0.11 m diameter case is longer than that found in the 0.15 m and 0.19 m diameter combustors. Therefore, if a Strouhal number collapse of the flame response is to be achieved, a more encompassing flame length needs to be established for the 0.11 m diameter combustor data.

ISSN No: 2348-4845
International Journal & Magazine of Engineering, Technology, Management and Research
A Peer Reviewed Open Access International Journal

Conclusions:

Results are presented from an experimental study of the effect of flame–wall interaction on the structure and response of lean-premixed swirl-stabilized flames. The experiments were conducted using a single-nozzle swirl-stabilized combustor con-figuration, with three different combustor diameters (0.11, 0.15, and 0.19 m), corresponding to confinement ratios (C_r) of 0.5, 0.37, and 0.29. Forced response measurements were taken over a range of operating conditions to characterize the effect of the lateral confinement on flame response in terms of the FTF.

Attempts to generalize the measured FTF data across all confinements by using the Strouhal number result in an imperfect collapse. Individual datasets can be normalized in terms of FTF extrema locations, but a generalization between combustor diame-ters is not achieved. Multiplying the Strouhal number by the con-finement ratio to account for the flow expansion ratio and to introduce the parameter $L_{f,CoHR}/D_{comb}$ into the normalization col-lapses the FTF data from the 0.15 m and 0.19 m diameter combus-tors but not data from the 0.11 m diameter combustor. This lack of collapse is attributed to a change in the flow field (free- to wall-jet from regime) and behavior of the flame in the smallest diameter combustor.

Heat release rate index images which detail the fluctuating flame structure as a function of confinement show that the flames in the smallest combustor became convectively noncompact at lower frequencies relative to flames in the larger diameter com-bustors with lower confinement. A change in the effective length of the flame, along with the fluctuating flame structure, is observed as confinement is increased and cited the cause of these differences.Chemiluminescence-based flame images show changes in over-all flame structure as the degree of flame–wall interaction is altered. Both the axial and radial distributions of the heat release rate from the flame are altered as the combustor diameter is changed.

In particular, as the lateral confinement is increased, the flame flattens against the combustor wall. This flattening of the flame is characterized using the FWHM of the axial heat release profiles of each flame. The parameter $L_{f,CoHR}/D_{comb}$ was introduced and used to scale data as a function of confinement. The use of this parameter has a physical basis in that it is representative of the flame base angle or aspect ratio, parameters that have been shown to govern flame response. Several flame metrics that vary with confinement are used to show that this parameter is indeed representative of the degree of flame–wall interaction experienced by the flame.

Acknowledgment:

Mr. **J MURALI NAIK, M.Tech (Ph.D)** Avanthi Institute of Engineering and technology, Dept. of Mechanical Engineer, was gratefully acknowledged for guiding to the test facility used in this study.

References:

[1] Lieuwen, T., 2005, "Nonlinear Kinematic Response of Premixed Flames to Harmonic Velocity Disturbances," Proc. Combust. Inst., 30(2), pp. 1725–1732.

[2] Huang, Y., and Yang, V., 2009, "Dynamics and Stability of Lean-Premixed Swirl-Stabilized Combustion," Prog. Energy Combust. Sci., 35(4), pp. 293–364.

[3] Fanaca, D., Alemela, P. R., Ettner, F., Hirsch, C., Sattelmayer, T., and Schuer-mans, B., 2008, "Determination and Comparison of the Dynamic Characteris-tics of a Perfectly Premixed Flame in Both Single and Annular Combustion Chambers," ASME Paper No. GT2008-50781.

[4] Merk, H. J., 1957, "An Analysis of Unstable Combustion of Premixed Gases," Symp. (Int.) Combust., 6(1), pp. 500–512.

ISSN No: 2348-4845
International Journal & Magazine of Engineering, Technology, Management and Research
A Peer Reviewed Open Access International Journal

[5] Jones, B., Lee, J. G., Quay, B. D., and Santavicca, D. A., 2011, "Flame Response Mechanisms Due to Velocity Perturbations in a Lean Premixed Gas Turbine Combustor," ASME J. Eng. Gas Turbines Power, 133(2), p. 021503.

[6] Kim, K. T., and Santavicca, D. A., 2013, "Interference Mechanisms of Acoustic/ Convective Disturbances in a Swirl-Stabilized Lean-Premixed Combustor," Combust. Flame, 160(8), pp. 1441–1457.

[7] Renard, P.-H., Thevenin, D., Rolon, J., and Candel, S., 2000, "Dynamics of Flame/Vortex Interactions," Prog. Energy Combust. Sci., 26(3), pp. 225–282.

[8] Ducruix, S., Schuller, T., Durox, D., and Sebastien, C., 2003, "Combustion Dynamics and Instabilities: Elementary Coupling and Driving Mechanisms," J. Propul. Power, 19(5), pp. 722–734.

[9] Bunce, N. A., Quay, B. D., and Santavicca, D. A., 2014, "Interaction Between Swirl Number Fluctuations and Vortex Shedding in a Single-Nozzle Turbulent Swirling Fully-Premixed Combustor," ASME J. Eng. Gas Turbines Power, 136(2), p. 021503.

[10] Palies, P., Durox, D., Schuller, T., and Candel, S., 2010, "The Combined Dynamics of Swirler and Turbulent Premixed Swirling Flames," Combust. Flame, 157(9), pp. 1698–1717.

[11] Syred, N., 2006, "A Review of Oscillation Mechanisms and the Role of the Precessing Vortex Core (PVC) in Swirl Combustion Systems," Prog. Energy Combust. Sci., 32(2), pp. 93–161.

[12] Fureby, C., Grinstein, F., Li, G., and Gutmark, E., 2007, "An Experimental and Computational Study of a Multi-Swirl Gas Turbine Combustor," Proc. Com-bust. Inst., 31(2), pp. 3107–3114.

[13] Szedlmayer, M. T., Quay, B. D., Samarasinghe, J., De Rosa, A., Lee, J. G., and Santavicca, D. A., 2011, "Forced Flame Response of a Lean Premixed Multi-Nozzle Can Combustor," ASME Paper No. GT2011-46080.

[14] Fanaca, D., Alemela, P., Hirsch, C., and Sattelmayer, T., 2010, "Comparison of the Flow Field of a Swirl Stabilized Premixed Burner in an Annular and a Sin-gle Burner Combustion Chamber," ASME J. Eng. Gas Turbines Power, 132(7), p. 071502.

[15] Samarasinghe, J., Peluso, S., Szedlmayer, M., De Rosa, A., Quay, B., and Santa-vicca, D., 2013, "Three-Dimensional Chemiluminescence Imaging of Unforced and Forced Swirl-Stabilized Flames in a Lean Premixed Multi-Nozzle Can Combustor," ASME J. Eng. Gas Turbines Power, 135(10), p. 101503.

[16] Hauser, M., Hirsch, C., and Sattelmayer, T., 2011, "Influence of the Confine-ment on the Flame Transfer Function," 18th International Congress on Sound and Vibration, Rio de Janeiro, Brazil, July 10–14, pp. 10–14.

[17] Szedlmayer, M. T., 2013, "An Experimental Study of the Velocity-Forced Flame Response of a Lean-Premixed Multi-Nozzle Can Combustor for Gas Turbines," Ph.D. thesis, The Pennsylvania State University, State College, PA.

[18] Birbaud, A., Durox, D., Ducruix, S., and Candel, S., 2007, "Dynamics of Confined Premixed Flames Submitted to Upstream Acoustic Modulations," Proc. Combust. Inst., 31(1), pp. 1257–1265.

[19] Birbaud, A. L., Durox, D., and Candel, S., 2007, "Dynamics of Unstable Premixed Flames

Under Variable Lateral Confinement Ratios," European Com-bustion Meeting, Chania, Crete, Apr. 11–13.

[20] Cuquel, A., Durox, D., and Schuller, T., 2013, "Scaling the Flame Transfer Function of Confined Premixed Conical Flames," Proc. Combust. Inst., 34(1), pp. 1007–1014.

[21] Fu, Y., Cai, J., Jeng, S.-M., and Mongia, H., 2005, "Confinement Effects on the Swirling Flow of a Counter-Rotating Swirl Cup," ASME Paper No. GT2005-68622.

[22] Tay-Wo-Chong, L., and Polifke, W., 2013, "Large Eddy Simulation-Based Study of the Influence of Thermal Boundary Condition and Combustor Confine-ment on Premix Flame Transfer Functions," ASME J. Eng. Gas Turbines Power, 135(2), p. 021502.

[23] Kedia, K., Altay, H., and Ghoniem, A., 2011, "Impact of Flame–Wall Interac-tion on Premixed Flame Dynamics and Transfer Function Characteristics," Proc. Combust. Inst., 33(1), pp. 1113–1120.

[24] Durox, D., Schuller, T., Noiray, N., and Candel, S., 2009, "Experimental Analy-sis of Nonlinear Flame Transfer Functions for Different Flame Geometries," Proc. Combust. Inst., 32(1), pp. 1391–1398.

[25] Kim, D., Lee, J. G., Quay, B. D., Santavicca, D. A., Kim, K., and Srinivasan, S., 2010, "Effect of Flame Structure on the Flame Transfer Function in a Premixed Gas Turbine Combustor," ASME J. Eng. Gas Turbines Power, 132(2), p. 021502.

[26] Lee, J. G., Gonzalez, E., and Santavicca, D. A., 2005, "On the Applicability of Chemiluminescence to the Estimation of Unsteady Heat-Release During Unstable Combustion in Lean Premixed Combustor," AIAA Paper No. 2005-3575.

[27] Clark, T. P., 1958, "Studies of OH, CO, CH, and C_2 Radiation from Laminar and Turbulent Propane-Air and Ethylene-Air Flames," National Advisory Com-mittee for Aeronautics. Lewis Flight Propulsion Laboratory, Cleveland, OH, NACA Technical Report No. 4266, NACA.

[28] Fleifil, M., Annaswamy, A., Ghoneim, Z., and Ghoniem, A., 1996, "Response of a Laminar Premixed Flame to Flow Oscillations: A Kinematic Model and Thermoacoustic Instability Results," Combust. Flame, 106(4), pp. 487–510.

[29] Balachandran, R., Ayoola, B., Kaminski, C., Dowling, A., and Mastorakos, E., 2005, "Experimental Investigation of the Nonlinear Response of Turbulent Premixed Flames to Imposed Inlet Velocity Oscillations," Combust. Flame, 143(1), pp. 37–55.

[30] Armitage, C., Balachandran, R., Mastorakos, E., and Cant, R., 2006, "Investigation of the Nonlinear Response of Turbulent Premixed Flames to Imposed Inlet Velocity Oscillations," Combust. Flame, 146(3), pp. 419–436.

[31] Birbaud, A., Ducruix, S., Durox, D., and Candel, S., 2008, "The Nonlinear Response of Inverted V Flames to Equivalence Ratio Nonuniformities," Combust. Flame, 154(3), pp. 356–367.

[32] Abom, M., and Boden, H., 1988, "Error Analysis of Two-Microphone Measure-ments in Ducts With Flow," J. Acoust. Soc. Am., 83(6), pp. 2429–2438.

[33] Waser, M. P., and Crocker, M. J., 1984, "Introduction to the Two-Microphone Cross-Spectral Method of Determining Sound Intensity," Noise Control Eng. J., 22(3), pp. 76–85.

[34] Vest, C., 1974, “Formation of Images From Projections: Radon and Abel Trans-forms,” JOSA, 64(9), pp. 1215–1218.

[35] Deans, S. R., 2007, The Radon Transform and Some of Its Applications, Courier Dover Publications, Mineola, NY.

[36] Bunce, N., Lee, J. G., Quay, B. D., and Santavicca, D. A., 2011, “Mixture-Forced Flame Transfer Function Measurements and Mechanisms in a Single-Nozzle Combustor at Elevated Pressure,” ASME Paper No. GT2011-46744.

[37] Schuermans, B., Bellucci, V., Guethe, F., Meili, F., Flohr, P., and Paschereit, C. O., 2004, “A Detailed Analysis of Thermoacoustic Interaction Mechanisms in a Turbulent Premixed Flame,” ASME Paper No. GT2004-53831.

[38] Poinsot, T. J., Trouve, A. C., Veynante, D. P., Candel, S. M., and Esposito, E. J., 1987, “Vortex-Driven Acoustically Coupled Combustion Instabilities,” J. Fluid Mech., 177, pp. 265–292

[39] Kim, K., and Santavicca, D., 2013, “Generalization of Turbulent Swirl Flame Transfer Functions in Gas Turbine Combustors,” Combust. Sci. Technol., 185(7), pp. 999–1015.

[40] Schuller, T., Durox, D., Cuquel, A., Palies, P., Moeck, J., and Candel, S., 2012, “Modeling the Response of Premixed Flame Transfer Functions—Key Ele-ments and Experimental Proofs,” AIAA Paper No. 2012-0985.

[41] Duchaine, F., Boudy, F., Durox, D., and Poinsot, T., 2011, “Sensitivity Analysis of Transfer Functions of Laminar Flames,” Combust. Flame, 158(12), pp. 2384–2394.

[42] Marble, F., and Candel, S., 1977, “Acoustic Disturbance From Gas Non-Uniformities Convected Through a Nozzle,” J. Sound Vib., 55(2), pp. 225–243.